Bves and NDRG4 regulate directional epicardial cell migration through autocrine extracellular matrix deposition

Emily C. Benesh[a,b], Paul M. Miller[a], Elise R. Pfaltzgraff[a], Nathan E. Grega-Larson[a], Hillary A. Hager[a], Bong Hwan Sung[c], Xianghu Qu[d], H. Scott Baldwin[d], Alissa M. Weaver[c,e], and David M. Bader[f]

[a]Department of Cell and Developmental Biology, [c]Department of Cancer Biology, [d]Department of Pediatric Cardiology, [e]Department of Pathology, and [f]Department of Medicine, Division of Cardiovascular Medicine, Vanderbilt University School of Medicine, Nashville, TN 37232; [b]Department of Obstetrics and Gynecology, Washington University in St. Louis, St. Louis, MO 63110

ABSTRACT **Directional cell movement is universally required for tissue morphogenesis. Although it is known that cell/matrix interactions are essential for directional movement in heart development, the mechanisms governing these interactions require elucidation. Here we demonstrate that a novel protein/protein interaction between blood vessel epicardial substance (Bves) and N-myc downstream regulated gene 4 (NDRG4) is critical for regulation of epicardial cell directional movement, as disruption of this interaction randomizes migratory patterns. Our studies show that Bves/NDRG4 interaction is required for trafficking of internalized fibronectin through the "autocrine extracellular matrix (ECM) deposition" fibronectin recycling pathway. Of importance, we demonstrate that Bves/NDRG4-mediated fibronectin recycling is indeed essential for epicardial cell directional movement, thus linking these two cell processes. Finally, total internal reflectance fluorescence microscopy shows that Bves/NDRG4 interaction is required for fusion of recycling endosomes with the basal cell surface, providing a molecular mechanism of motility substrate delivery that regulates cell directional movement. This is the first evidence of a molecular function for Bves and NDRG4 proteins within broader subcellular trafficking paradigms. These data identify novel regulators of a critical vesicle-docking step required for autocrine ECM deposition and explain how Bves facilitates cell-microenvironment interactions in the regulation of epicardial cell–directed movement.**

Monitoring Editor
Josephine C. Adams
University of Bristol

Received: Aug 10, 2012
Revised: Aug 28, 2013
Accepted: Sep 11, 2013

This article was published online ahead of print in MBoC in Press (http://www.molbiolcell.org/cgi/doi/10.1091/mbc.E12-07-0539) on September 18, 2013.

The authors declare that they have no conflict of interest.

E.C.B., P.M.M., and D.M.B. conceived and designed the research; E.C.B., P.M.M., E.R.P., and N.E.G. performed the research; A.M.W., B.H.S., P.M.M., X.Q., and H.S.B. contributed reagents/materials/analysis tools; E.C.B., P.M.M., and D.M.B. analyzed the data; and E.C.B., P.M.M., and D.M.B. wrote the manuscript.

Address correspondence to: Alissa M. Weaver (alissa.weaver@vanderbilt.edu), David M. Bader (david.bader@vanderbilt.edu).

Abbreviations used: Bves, blood vessel epicardial substance; Bv/N4-MBD, Bves/NDRG4 minimal binding domain; ECM, extracellular matrix; NDRG4, N-myc downstream regulatory gene 4; SC, standard control; 3′UTR, 3′ untranslated region; VAMP3, vesicle-associated membrane protein 3.

INTRODUCTION

Blood vessel epicardial substance (Bves; or Popdc1), an integral membrane protein, is the prototypical member of the Popdc family, which regulates cell migration and adhesion through unknown molecular mechanisms. Bves shares a conserved cAMP-binding Popeye domain but contains no other homologous functional domains with other protein families (Andrée *et al.*, 2000; Froese *et al.*, 2012). First identified in epicardial tissue, Bves is now recognized for its dynamic distribution in a multitude of cell types (Reese *et al.*, 1999; Andrée *et al.*, 2000; DiAngelo *et al.*, 2001; Wada *et al.*, 2001; Ripley *et al.*, 2004; Vasavada *et al.*, 2004; Smith and Bader, 2006; Kawaguchi *et al.*, 2008; Russ *et al.*, 2010). Disruption of Bves randomizes and accelerates cell movement. For example, in normal *Xenopus laevis* development, individual A1 blastomeres, early embryonic cells, give rise to progeny that migrate in a highly patterned

manner, incorporating into anterior head and somitic structures. With morpholino knockdown of Bves in these same blastomeres, migration of resulting progeny is completely randomized, with cells moving throughout the embryo (Ripley *et al.*, 2006). Randomization of movement after Bves loss of function is a recurring theme observed in both single-cell and sheet epithelium migration models, including human corneal epithelial cells, germ cells of the fly, and myoblasts in murine skeletal muscle regeneration (Wada *et al.*, 2001; Andrée *et al.*, 2002; Ripley *et al.*, 2004, 2006; Osler *et al.*, 2005; Lin *et al.*, 2007; Kawaguchi *et al.*, 2008; Smith *et al.*, 2008; Hager *et al.*, 2010; Kim *et al.*, 2010). Bves function in regulation of cell movement is of immediate relevance, as Bves has recently been identified as a metastasis suppressor in colorectal cancers (Williams *et al.*, 2011). Thus Bves is an important mediator of cell adhesion and movement in a variety of settings.

Although Bves has emerged as a strong regulator of cell movement, the lack of identifiable motifs within the protein has made assignment of molecular functions challenging. To circumvent this problem, yeast two-hybrid interaction screens were conducted to identify binding partners and link Bves to a molecular function. Of importance, Hager *et al.* (2010) demonstrated that Bves interacts with the recycling endosome soluble *N*-ethylmaleimide–sensitive factor attachment protein receptor (SNARE) protein, vesicle-associated membrane protein 3 (VAMP3; cellubrevin), to facilitate trafficking of two canonical VAMP3-dependent cargoes, transferrin and β_1-integrin, to the cell surface. Previous work demonstrated that loss of Bves function disrupted subcellular localization of cell/cell adhesion molecules such as E-cadherin and occludin (Osler *et al.*, 2005; Russ *et al.*, 2011). Thus we postulated that Bves serves as a pivotal regulator of subcellular trafficking of molecules to the cell surface. Still, understanding of the precise molecular behavior of Bves within subcellular trafficking pathways remains unresolved.

Here using multiple methodologies, we identify a novel interaction between Bves and N-myc downstream regulated gene 4 (NDRG4), which is of interest because NDRG4 influences cell behaviors regulated by Bves, including cell migration and process extension (Zhou *et al.*, 2001; Qu *et al.*, 2002, 2008; Nishimoto *et al.*, 2003; Melotte *et al.*, 2009; Schilling *et al.*, 2009; Kim *et al.*, 2010; Williams *et al.*, 2011). Loss of NDRG4 in mouse models depletes intracerebral brain-derived neurotrophic factor through unknown mechanisms, causing spatial learning defects in animals (Yamamoto *et al.*, 2011). Thus it is intriguing that the NDRG protein family has been generally implicated in trafficking of cell surface proteins (Ohki *et al.*, 2002; Okuda *et al.*, 2004; Berger *et al.*, 2006; Kachhap *et al.*, 2007; Choi *et al.*, 2010). Finally, NDRG4, like Bves, is a colorectal cancer tumor suppressor (Melotte *et al.*, 2009). Owing to these functional similarities, the relationship between Bves and NDRG4 was analyzed in greater depth.

We demonstrate that Bves/NDRG4 protein function provides the molecular underpinning for two critical and previously unlinked cell behaviors in epicardial cells. First, our data determine that this interaction is essential for directional cell movement, as its disruption randomizes and accelerates cell migration. Next we demonstrate that Bves and NDRG4 regulate the deposition of internalized soluble fibronectin for resecretion through the autocrine extracellular matrix (ECM) recycling pathway (Sung *et al.*, 2011). Of importance, a series of cell/ECM recombination studies reveals that directional cell movement is, in fact, dependent on fibronectin recycling and that Bves/NDRG4 interaction is essential in linking these two processes. Further, live-cell imaging using total internal reflectance fluorescence (TIRF) microscopy reveals that Bves/NDRG4 interaction mediates cell surface docking of VAMP3-positive recycling endosomes. These data provide a molecular mechanism for motility substrate delivery that regulates directional cell movement. Taken together, they demonstrate that Bves, through interaction with its binding partners, is essential for cell surface fusion of endosomes in regulation of cell motility and adhesion. Given the diversity of phenotypes observed with Bves loss of function, the present study has broad implications for development, cancer, and repair.

RESULTS

Bves and NDRG4 bind directly through a novel interaction domain

In an effort to determine molecular function, were identified Bves binding partners with a split ubiquitin two-hybrid screen (Iyer *et al.*, 2005) designed for membrane-associated proteins using Bves as bait. Initial results identified a direct interaction between Bves and NDRG4 that passed all stringency selection tests (DualSystems, Biotech, Zurich, Switzerland). Myc-tagged full-length Bves (Bves-myc) coimmunoprecipitated with green fluorescent protein (GFP)–tagged NDRG4 (NDRG4-GFP) from Cos7 cell lysates, biochemically confirming the interaction identified by split ubiquitin screening technology (Figure 1A). To further define the interaction domain, we analyzed a series of glutathione *S*-transferase (GST)–tagged Bves constructs in which the C-terminus (GST-Bves357; amino acids 115–357) was successively truncated (Figure 1B, left). Only the GST-Bves357 interacted with NDRG4 (Figure 1B, right). All other C-terminal truncations failed to pull down NDRG4-GFP. All Bves-GST truncations failed to interact with enhanced GFP expressed in Cos7 cell lysates (Figure 1B′). These data suggested that the NDRG4 binding domain was likely to be contained within the region between amino acids 300 and 357.

SPOTs analysis (as modified from Kawaguchi *et al.*, 2008) was performed to determine the minimal Bves residues sufficient to interact with NDRG4. Thirteen-mer peptides of BCT were fused to a cellulose membrane with 10–amino acid overlap between adjacent peptides (diagram in Figure 1C) and probed with Cos7 lysate enriched for NDRG4-GFP. NDRG4-GFP specifically bound to peptides 63–65, which corresponded to residues 307–316 of the Bves protein (Figure 1C, bottom and overlay). Of importance, SPOTs analysis mirrored our truncation pull-down results, in which Bves/NDRG4 interaction was observed only with inclusion of residues 300–357 (Figure 1D). These data identify a novel protein–protein interaction site within the Bves C-terminus that is outside of the conserved Popeye domain. It is a region found only in Bves and not in Popdc2/3 (National Center for Biotechnology Information [www.ncbi.nlm.nih.gov/]; Popdc1/Bves [NP_077247.1]; Popdc2 isoforms 1 and 2 [NP_001075453.1, NP_071713.1]; Popdc3 [NP_077248.1]). The newly identified Bves/NDRG4 minimal binding domain (Bv/N4-MBD) was cloned into a Myc-tagged fusion vector (residues 292–331 cloned into Myc-3tag vector; Figure 1D).

Bves and NDRG4 colocalize and interact in mammalian epicardial cells

Bves and NDRG4 gene products are both enriched in the developing heart tube (Qu *et al.*, 2002; Hager and Bader, 2009). We examined the precise distribution patterns of the two proteins in E14.5 cardiac tissue and determined that Bves and NDRG4 colocalized in both epicardial cells and cardiac myocytes (Figure 2A, epicardium in inset). Furthermore, coimmunoprecipitation of epicardial cell lysates demonstrated that an antibody to endogenous Bves pulls down both Bves and NDRG4 protein, whereas MF-20 antibody, an anti–sarcomeric myosin heavy chain antibody (Bader *et al.*, 1982) bound to beads, did not (Figure 2B). Given that subcellular localization of Bves varies depending on whether cells are freely migratory or

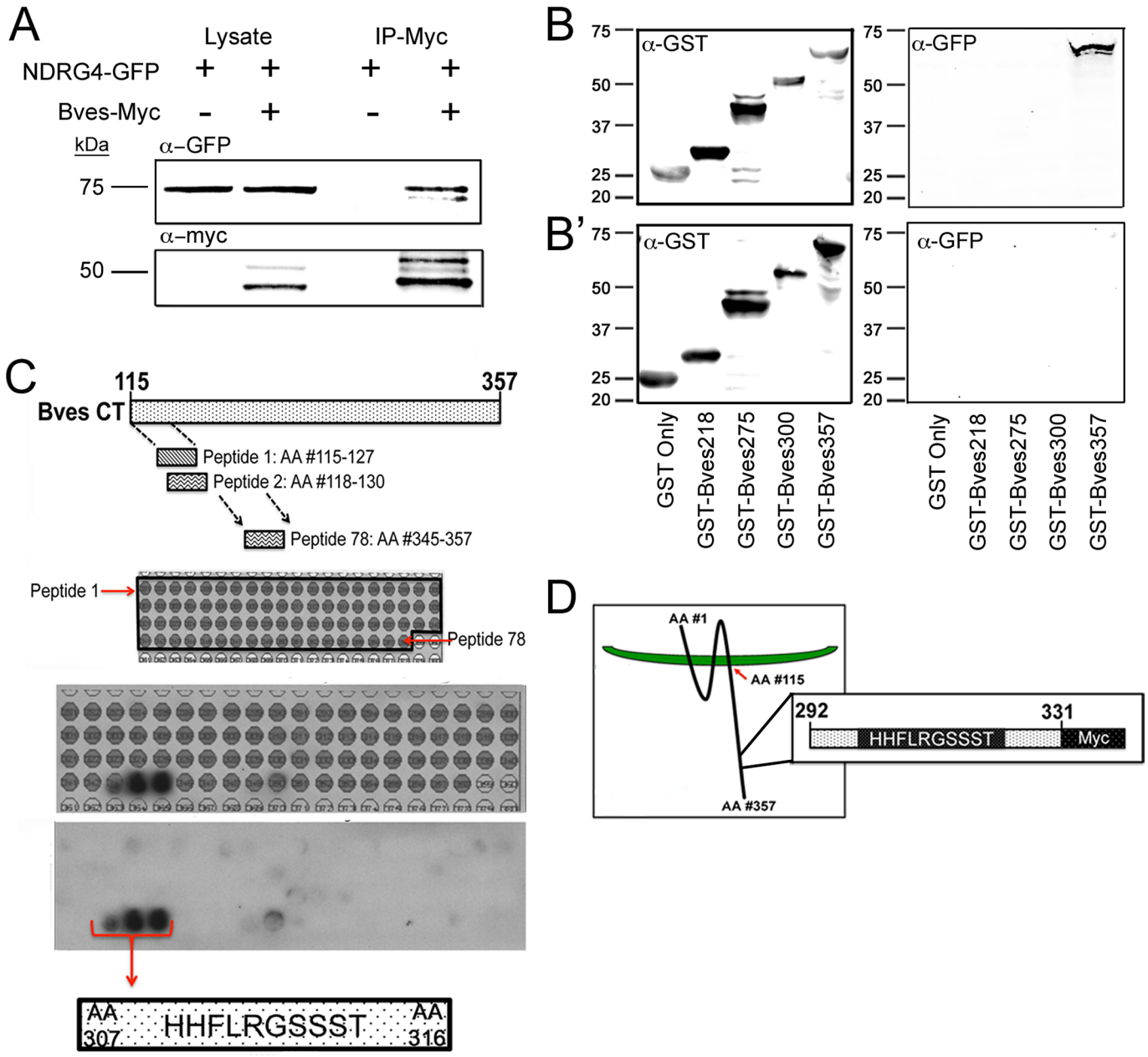

FIGURE 1: NDRG4 protein interacts with Bves residues 307–316. (A) Exogenously expressed Bves-Myc protein pulled down NDRG4-GFP. NDRG4-GFP did not pull down in the absence of Bves-Myc. (B) NDRG4-GFP was pulled down by GST-Bves357 (amino acids 115–357), whereas other truncations of GST-Bves357 (amino acids 115 to 218, 275, or 300, respectively) or GST-only control failed to pull down NDRG4-GFP. (B′) GFP-vector lysates fail to be pulled down by GST-Bves357 or other truncations. (C) In the SPOTs assay, 13-mer synthesized peptides from amino acid 115 to the end of the Bves protein were fused to a cellulose membrane, with 10–amino acid overlap between adjacent peptides. GFP-NDRG4 lysate binds to three consecutive Bves peptides on the cellulose membrane, peptides 63–65 (depicted in grid overlay), corresponding to Bves residues 307–316: HHFLRGSSST. (D) A domain from Bves residues 292–331, containing the Bv/N4-MBD identified in C, is cloned into the myc-3tag vector. $n \geq 4$ assays/experiment.

within epithelial sheets (Wada *et al.*, 2001; Osler *et al.*, 2005), we examined the subcellular localization of Bves and NDRG4 under varied epicardial cellular conditions. Epicardial cells at low confluence are motile, with a mesenchymal morphology (Wada *et al.*, 2003). In this setting, Bves and NDRG4 colocalized at the cell cortex, in extended cell processes (Figure 2C, inset and intensity profile), and on intracellular, vesicle-like structures (Figure 2D, digital zoom and white arrows). In other regions, nonoverlapping distribution of these proteins was also apparent. Of interest, the proteins failed to colocalize in established epicardial sheets (Figure 2E, inset). Here NDRG4 localization was primarily cytoplasmic, whereas Bves localized to the cell cortex and plasma membrane. Fluorescence was not apparent in secondary antibody-only negative controls, demonstrating that the signal was the result of anti-Bves and anti-NDRG4 antibody activity (Supplemental Figure S1). Taken together, these data indicate that Bves and NDRG4 interact in epicardial cells. Colocalization in cells of motile morphology suggests that Bves and NDRG4 function in a capacity related to cell migration.

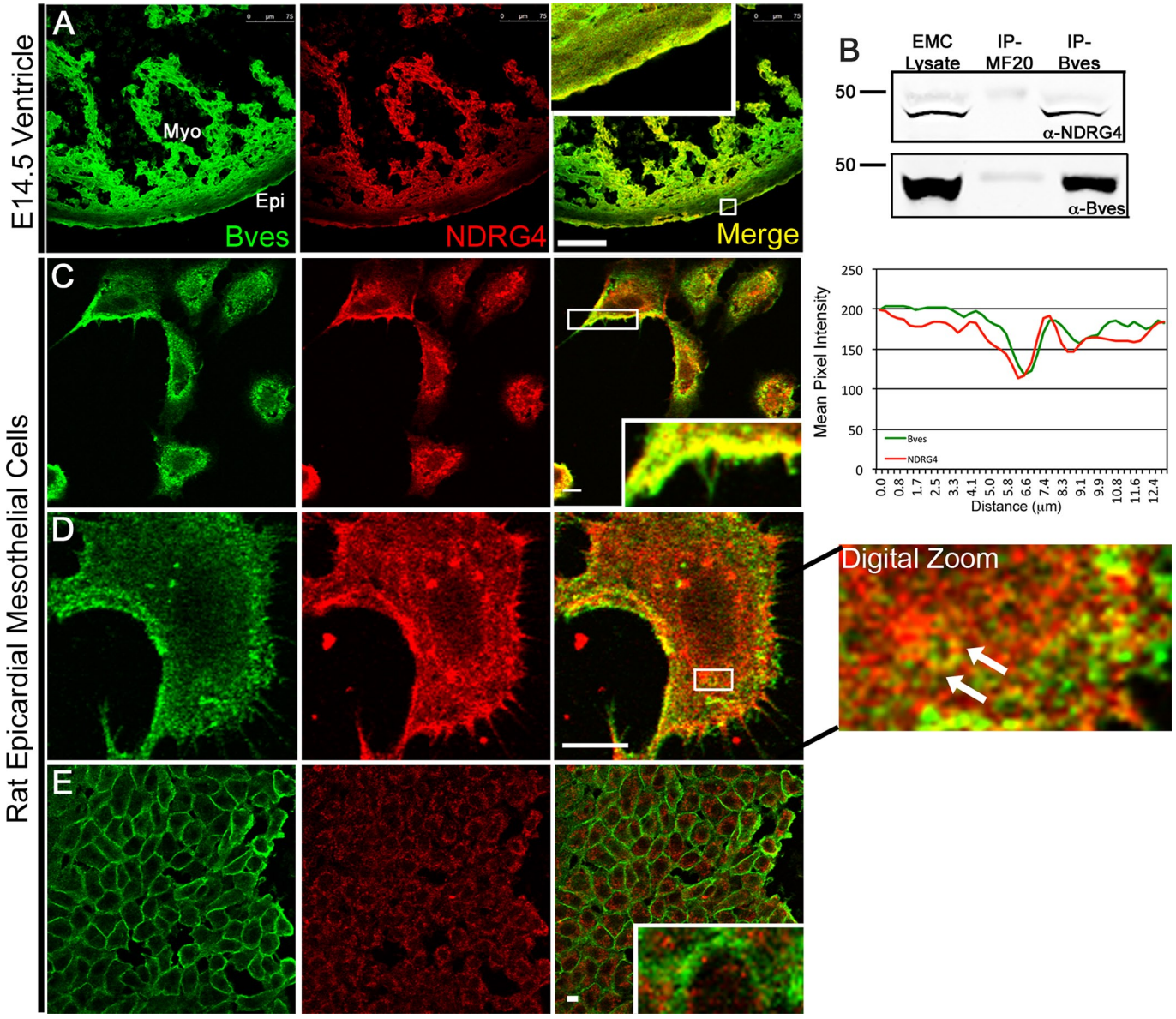

FIGURE 2: Bves and NDRG4 colocalize and interact in mammalian epicardial cells. (A) Bves and NDRG4 colocalize in trabecular cardiomyocytes (merge) and epicardial cells (box denotes digitally zoom inset) from E14.5 murine heart sections. Scale, 75 μm. (B) A column cross-linked to Bves antibody pulls down NDRG4 protein from epicardial cell lysate, whereas another antibody, MF-20, does not; $n \geq 4$ pull downs. (C) Epicardial cells at low confluence exhibit Bves and NDRG4 colocalization in plasma membrane protrusions (box denotes digitally zoomed inset); graph depicts colocalization in confocal images (D). Punctate, vesicle-like colocalization of Bves and NDRG4 are apparent in high-magnification confocal images of epicardial cells with motile morphology (box denotes digitally zoomed inset; white arrows demarcate vesicle-like structure). (E) Bves/NDRG4 fail to colocalize in confocal images of epicardial cell sheets (box denotes inset of cell borders). Epi, epicardium; Myo, myocardium; optical slices, 1 AU. Colocalizations quantified by ImageJ intensity profiling, Bar, 10 μm or as marked.

Bves and NDRG4 interaction regulates epicardial cell movement

To ascertain whether Bves and/or NDRG4 regulated cell motility in epicardial cells, we disrupted protein expression by two independent assays: 1) delivery of small interfering RNA (siRNA) to deplete cells of either/both proteins, and 2) application of the Bves/NDRG4 minimal-binding domain construct (Bv/N4-MBD) to specifically disrupt the Bves/NDRG4 interaction. Both NDRG4 (Figure 3A) and Bves (Figure 3B) oligos depleted each protein, whereas partner protein expression was not significantly affected (Figure 3, A–B′). As expected, pooling NDRG4 and Bves oligos visibly depleted both proteins (Figure 3, A and B). The average band intensity from three blots normalized to cyclophilin indicated that the NDRG4 (Figure 3A′), Bves (Figure 3B′), and pooled oligo (Figure 3, A′ and B′) depletions were significantly and highly reduced relative to standard control treatments. In addition, Bv/N4-MBD was tested for interference with native Bves and NDRG4 binding. Bv/N4-MBD proteins overexpressed in epicardial cells exhibited cytoplasmic localization, consistent with native NDRG4 (Figure 3C compared with Figure 2D). Single-pixel confocal analysis of all *z*-planes revealed that Bv/N4-MBD and native NDRG4 proteins colocalized in epicardial cells (Figure 3, D, cells, and E, single-pixel colocalization). Analysis of

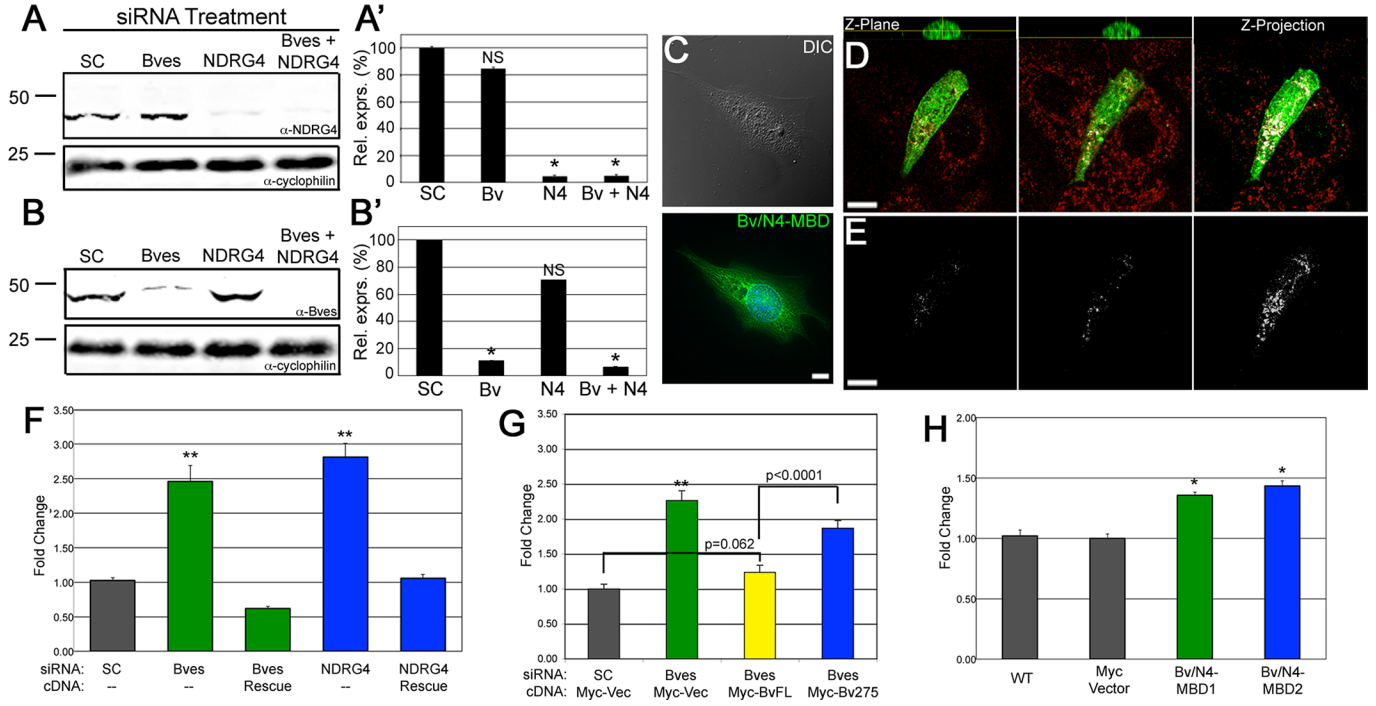

FIGURE 3: The Bves and NDRG4 interaction regulates epicardial cell movement. 3′UTR targeting NDRG4 and Bves oligos specifically reduce protein levels of each gene, respectively (A, B). Cyclophilin blots are protein loading controls (α-cyclophilin). (A′) Densitometry analysis of three blots demonstrates significant depletion of NDRG4 from NDRG4 and Bves + NDRG4 siRNA–treated epicardial cells (graphs relative to SC levels; $p < 0.05$; NS, not significant). (B′) Significant depletion of Bves is demonstrated from three blots in Bves and Bves + NDRG4 siRNA–treated epicardial cells (*$p < 0.05$; NS, not significant). (C) Overexpressed Bv/N4-MBD localizes in cytoplasmic puncta in epicardial cells. Bar, 10 μm. (D) Single-pixel colocalization of the Bv/N4-MBD construct (green) with native NDRG4 protein (red) in multiple *Z*-planes is (E) demarcated by white pixels (0.5-μm optical slices; bar, 10 μm). (F) Random epicardial transwell migration is elevated with Bves/NDRG4 siRNA treatment and rescued by stable overexpression of each gene. (G) Expression of Bves-full length plasmid (Myc-BvFL) rescues transwell migration of epicardial cells expressing Bves siRNA, whereas expression of a Bves plasmid truncated at residue 275 (Myc-Bv275) does not. (H) Overexpression of two clones of the Bv/N4-MBD construct (Bv/N4-MBD1 and 2, respectively) induces an increase in random cell motility due to disruption of Bves–NDRG4 interaction. For F–H, $n \geq 3$ assays/experiment, *$p \leq 0.05$, **$p \leq 0.0003$, from SCs.

average band intensities indicated that Bv/N4-MBD pulled down NDRG4-GFP significantly more than GFP-vector controls, despite higher expression of GFP-vector per 25 μg of Cos7 lysate (Supplemental Figure S2, A and A′; compare cyclophilin loading control to GFP expression in lysate). In addition, overexpression of Bv/N4-MBD interfered with the native interaction of Bves and NDRG4 protein as assessed by endogenous pull-down assay (Supplemental Figure S2B). Together these data demonstrate that Bves and NDRG4 protein levels can be significantly and predictably reduced with siRNA constructs. In addition, overexpressed Bv/N4-MBD interacts with native NDRG4 and interferes with endogenous Bves/NDRG4 binding.

With successful depletion of protein levels, we assayed whether loss of Bves and/or NDRG4 affected epicardial cell migration. Knockdown cells were placed within a modified Boyden chamber in which serum chemoattractant was homogeneously distributed on both sides of the filter to promote random motility. siRNA depletion of Bves or NDRG4 significantly increased random movement of epicardial cells (Figure 3F). This phenotype was rescued by stable coexpression of Bves or NDRG4 DNA lacking the 3′-untranslated region (3′UTR) oligonucleotide target sequences (Figure 3F). Next we determined whether the Bves/NDRG4 minimal-binding domain regulates undirected epicardial cell movements. First, we expressed Bves siRNAs as in Figure 3F to elevate random migration. Transient coexpression of Bves full-length plasmid completely rescued undirected migration of epicardial cells back to control levels (Figure 3G). Of importance, transient coexpression of the Bves truncation mutant (myc-Bves275) lacking the NDRG4 interaction domain failed to rescue the number of randomly migrating cells (Figure 3G). Finally, overexpression of two separate Bv/N4-MBD plasmid clones significantly increased transwell migration compared with controls (Figure 3H), corroborating gene depletion studies. Taken together, these data demonstrate that Bves and NDRG4 interaction regulates undirected migration in epicardial cells.

Bves/NDRG4 interaction regulates epicardial cell directional persistence and fibronectin trafficking

Disruption of Bves/NDRG4 interaction increases random cell movement, but the underlying molecular and cellular mechanisms are not understood. To observe the specific motility defect impaired with loss of Bves and/or NDRG4 function, we treated epicardial cells with Bves and/or NDRG4, or standard control (SC) siRNA, plated on glass in complete medium, and imaged for 2 h at a frame rate of 1/min (SC, Supplemental Movie S1; Bves/NDRG4 depleted, Supplemental Movie S2; Bves depleted, Supplemental Movie S3; NDRG4 depleted, Supplemental Movie S4). Distance traveled, velocity, and directional persistence were quantified using ImageJ manual tracking analysis (Figure 4, A and B; demarcated by colored lines overlaid on movies and stills). Depleted cells exhibited significantly increased velocity and path lengths as compared with controls (Figure 4C and

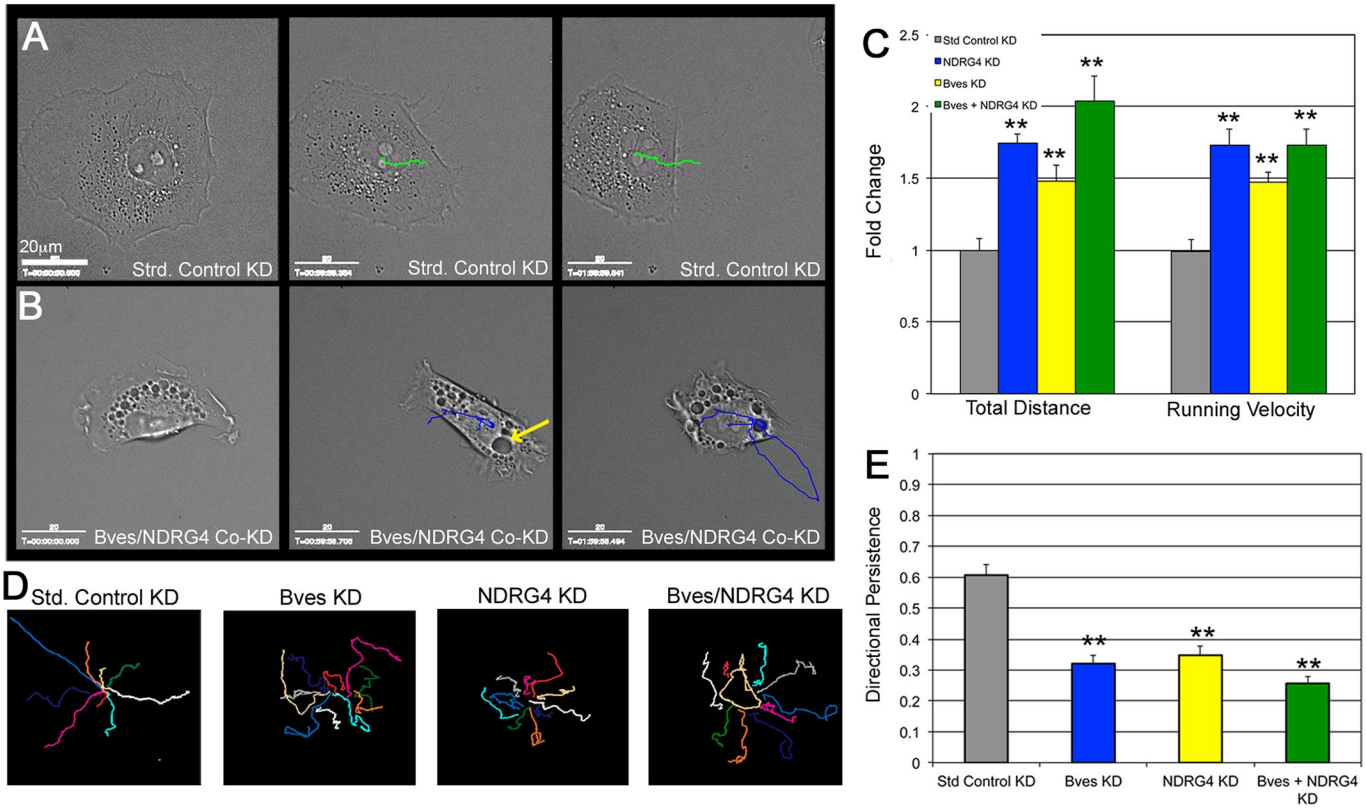

FIGURE 4: Bves and NDRG4 coregulate epicardial cell directional persistence and fibronectin trafficking. Lines overlaid on time-lapse movies using manual tracking analysis (ImageJ) demarcate cell movements per minute. (A) The migration pattern of epicardial cells treated with SC siRNAs is directional. (B) The migration pattern of Bves/NDRG4 co-knockdown epicardial cells shows increased distance traveled and lacks directionality compared with controls. Cells also retain large cytoplasmic vacuoles (yellow arrow). (C) Bves and/or NDRG4 knockdown causes significantly accelerated cell movement speed and increased distance traveled. (D) An overlay of 10 representative tracks of cells illustrates the randomized cell movements due to Bves and/or NDRG4depletion. Scale bars, 20 μm; $n \geq 40$ cells/condition. (E) Directional persistence is highly impaired in Bves- and/or NDRG4-depleted epicardial cells (1 = highly directional, 0 = random); $^{**}p \leq 0.001$.

Supplemental Figure S3A). An overlay of the progressive paths of 10 representative cells visually demonstrates that disruption of Bves and/or NDRG4 function randomizes cell movement (Figure 4D). Of interest, quantitation of the data revealed that Bves-depleted, NDRG4-depleted, or codepleted cells had strikingly poor directional persistence (Figure 4E). Directional persistence is calculated by dividing the total displacement by the distance traveled; it is measured on a scale of 0 to 1, where 0 is random movement and 1 is movement in a straight line (Harms *et al.*, 2005). Treatment of epicardial cells with Bv/N4-MBD also significantly impaired directional persistence, mimicking siRNA knockdown results. Distance traveled and velocity were also statistically significantly increased, albeit more modestly than with protein deletion (Supplemental Figure S3, C and D).

In addition to impaired cell movements, time-lapse differential interference contrast imaging demonstrated that Bves- and/or NDRG4-depleted cells accumulated large cytoplasmic vacuoles (Figure 4B, yellow arrow) that originated at the plasma membrane and rapidly traveled toward the nucleus (exemplified in Supplemental Movies S2 and S3). Because vesicular enlargement is generally associated with membrane-trafficking defects (Neufeld *et al.*, 2004), this finding suggested that presence of Bves and NDRG4 proteins is necessary for regulation of vesicular transport. Our previous data demonstrate that vesicular trafficking of exogenous fibronectin present in the environment influences cell movement (Sung *et al.*, 2011). Given the current phenotype of randomized cell movement and defective vesicular trafficking, we tested whether fibronectin accumulated intracellularly in Bves- and/or NDRG4-depleted cells.

Immunofluorescence confocal microscopy revealed that large fibronectin-positive structures are indeed present in the cytoplasm of these cells (Figure 5A; DiI lipophilic dye labels cell borders). Quantification by object analysis using ImageJ revealed that Bves- and/or NDRG4-depleted cells exhibited a twofold to threefold increase in the number, mean area, and intensity of fibronectin-positive structures compared with controls (Figure 5, B and C). Similarly, application of Bv/N4-MBD (compared with GFP-vector transfection control) induced retention of Dylight-550 labeled fibronectin, which was supplemented in fibronectin-depleted medium (Figure 5D). The size, number, and intensity of these internal fibronectin-positive compartments mirrored what was seen with endogenous fibronectin retention after siRNA knockdown (Figure 5B). Immunostaining demonstrated that fibronectin accumulated in LAMP2-positive endosomal/lysosomal compartments (Figure 5E) and small Rab11a-positive endosomes (Figure 5F). Together these data demonstrate that disruption of Bves and NDRG4 function impairs endocytic trafficking of fibronectin.

Fibronectin substrate rescues Bves and NDRG4 migration and trafficking defects

It was previously demonstrated that migration defects in cells deficient in autocrine ECM production can be fully rescued by

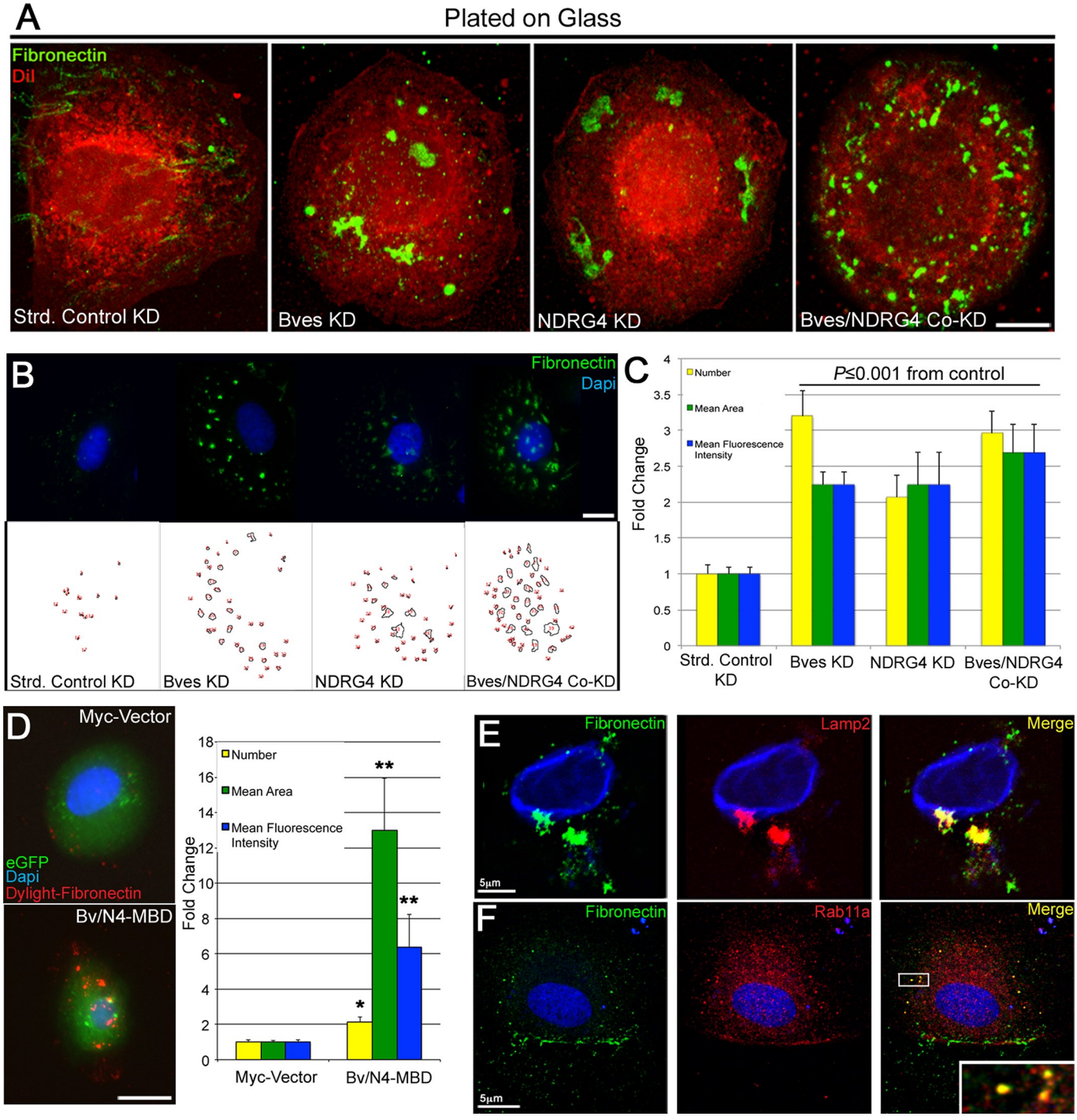

FIGURE 5: Bves/NDRG4-depleted cells contain large fibronectin-positive objects in late endosomal/lysosomal and recycling endosome compartments. (A) Endogenous fibronectin-positive cytoplasmic objects are apparent in Bves- and/or NDRG4-depleted epicardial cells (DiI, red; fibronectin antibody, green). (B, C) Objects were measured using ImageJ particle analysis (top, original image; bottom, included particles). Bves- and/or NDRG4-depleted cells have significantly more fibronectin-positive objects that are larger with stronger fluorescence intensity compared with SC. (D) Bv/N4-MBD epicardial cells demonstrate increased number of internalized cytoplasmic DyLight-fibronectin 550 granules that are larger, with stronger fluorescence intensity compared with controls, *$p \leq 0.001$, **$p \leq 0.0001$, from respective control cells. (E) Bves/NDRG4-depleted epicardial cells exhibit fibronectin-positive objects (green) traffic in late endosomal/lysosomal compartments labeled with Lamp2 (red) in. Bar, 5 μm. (F) Fibronectin-positive objects (green) are also apparent in recycling endosomes labeled with Rab11a (red; box denotes inset) in these cells. Scale bars, 10 μm unless otherwise indicated, $n \geq 50$ cells/condition; optical slices, 1 AU.

supplying high concentrations of exogenous ECM substrate (Sung *et al.*, 2011). Thus, to determine whether Bves and NDRG4 regulate fibronectin recycling, Bves-depleted, NDRG4-depleted, and codepleted cells were plated on glass coverslips coated with 10 μg/ml fibronectin and assayed by live imaging as in Figure 4 (SC, Supplemental Movie S5; Bves/NDRG4 depleted,

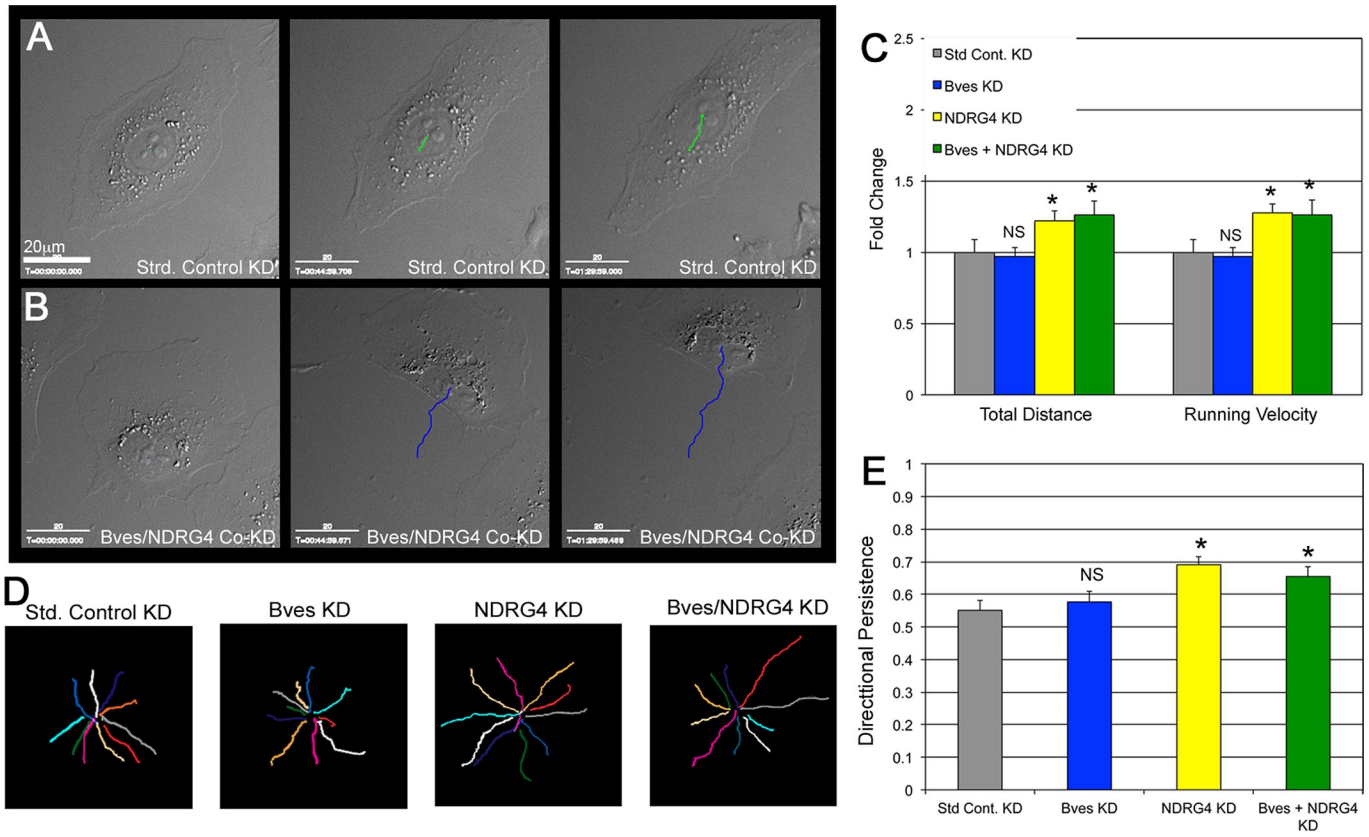

FIGURE 6: Homogeneous fibronectin substrate rescues Bves and NDRG4 migration defects. Epicardial cells are imaged and tracked as in Figure 4. Highly directional movement of SC-treated (A) epicardial cells is apparent on an evenly distributed fibronectin substrate as well as in Bves/NDRG4-codepleted cells (B) over a 2-h time course. (C) Migration distance and velocity of Bves- and/or NDRG4-depleted epicardial cells are only partially restored on fibronectin substrate. (D) Epicardial cells exhibit highly directional movement on fibronectin substrates regardless of siRNA treatment condition, as represented by 10 paths stacked together. Scale bars, 20 μm. *$p \leq 0.05$; $n \geq 44$ cells/condition; NS, not significant. (E) Bves-depleted cell directionality is fully rescued by fibronectin substrates as calculated by directional persistence quantifications. NDRG4/Bves codepleted cells exhibit improved directionality compared with controls. $n = 3$ experiments/condition; *$p < 0.05$.

Supplemental Movie S6; Bves depleted, Supplemental Movie S7; NDRG4 depleted, Supplemental Movie S8). Of interest, Bves- and/or NDRG4-depleted cells migrated with strong directional persistence equivalent to or improved beyond SC levels when plated on a fibronectin substrate, unlike the randomized movements observed on glass (Figure 6, C and E, and Supplemental Figure S3B). In addition, Bv/N4-MBD was applied to epicardial cells, and migration was assessed on fibronectin substrate. Similar to gene-depletion studies, Bv/N4-MBD–induced directional persistence defects were completely rescued by fibronectin substrate (Supplemental Figure S3C). Intriguingly, distance and velocity measurements in NDRG4-depleted and codepleted cells were only partially rescued by plating on exogenous fibronectin, whereas migration distance and velocities were not rescued at all in Bv/N4-MBD–expressing cells (Figures 6C and Supplemental Figure S3D). These data suggest that secretion of matrix dependent on Bves, and NDRG4 is specifically responsible for directional persistence, whereas other migration characteristics either may depend on different secretory cargo or require alternative Bves and/or NDRG4 functions. Overall, exogenously applied fibronectin matrix rescued directionality, suggesting that a key function of the Bves–NDRG4 interaction may be to regulate fibronectin recycling to facilitate directional movement.

Bves and NDRG4 regulate autocrine ECM deposition

Our data suggest that Bves and NDRG4 regulate cell movement through fibronectin recycling. To test the functionality of ECM produced by control and Bves/NDRG4-depleted cells, we isolated autocrine-produced, cell-free ECM from each of the cell types by removing confluent cell monolayers with 20 mM ammonium hydroxide (Sung *et al.*, 2011). Fresh Bves/NDRG4-depleted or SC-treated cells were then plated on these cell-free matrices and monitored for directional persistence for 2 h. On ECM produced by control cells, newly plated epicardial cells moved directionally whether cells were treated with SC or Bves/NDRG4 siRNA (Figure 7, A and A′; SC cells, Supplemental Movie S9; Bves/NDRG4-depleted cells, Supplemental Movie S10). This is similar to results obtained from cells plated on exogenous fibronectin substrates (Figure 6B). In contrast, only control cells moved in a directionally persistent manner on ECM produced by Bves/NDRG4-depleted cells (Figure 7, A and A′; SC cells, Supplemental Movie S11; Bves/NDRG4-depleted cells, Supplemental Movie S12), whereas Bves/NDRG4-depleted cells moved randomly, phenocopying their behavior on matrix-free glass (Figure 4B).

In this experiment, soluble fibronectin was present in the medium in both experimental conditions. Thus a possible explanation for the efficient migration of control cells on matrix produced by Bves/NDRG4-depleted cells is that control cells can dynamically

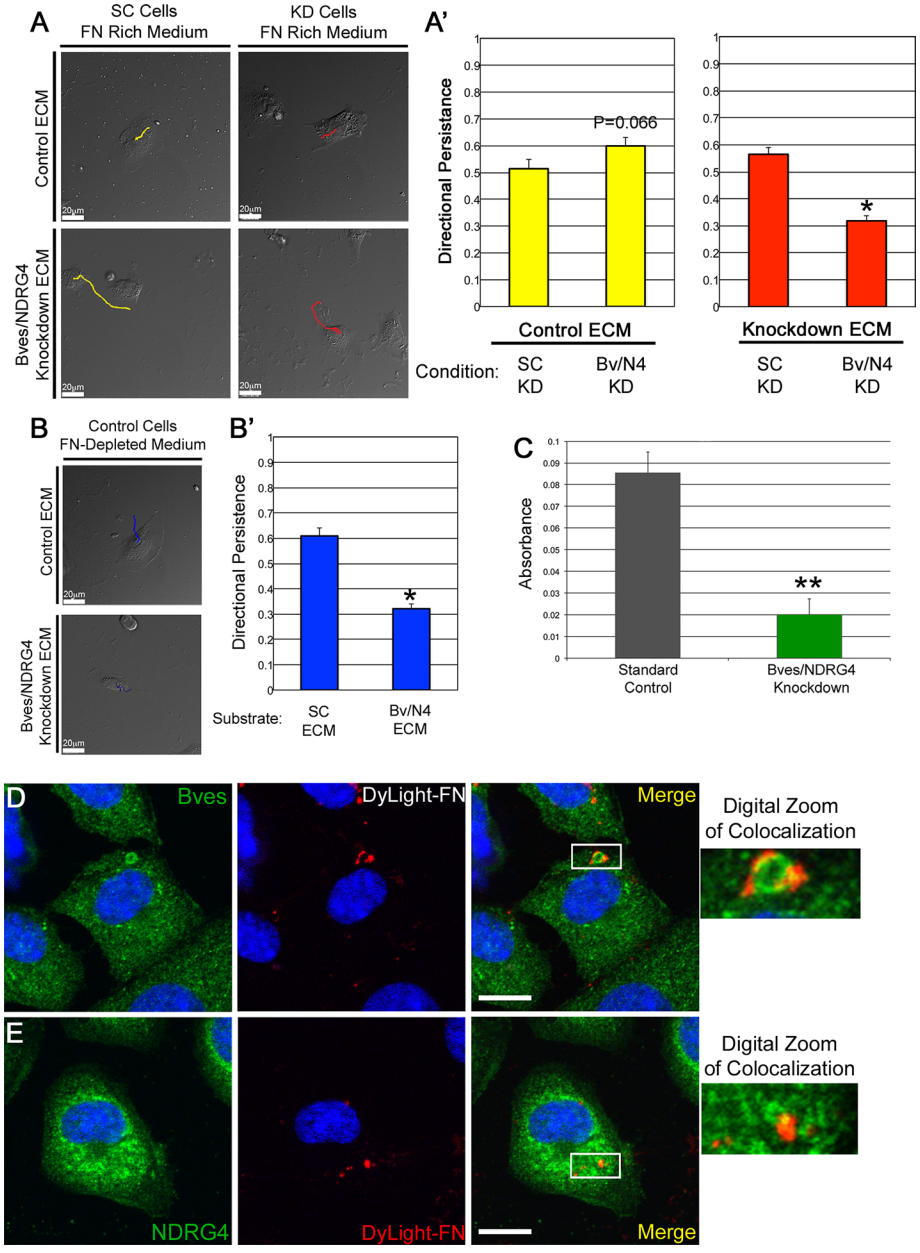

FIGURE 7: Bves and NDRG4 coregulate fibronectin deposition. Matrix deposition is probed using a cell-free ECM assay, which removes cells but keeps the ECM. Migration of newly plated cells is then tracked as in Figures 4 and 6 on previously produced ECM to test the function of residual matrix. (A) On control-produced ECM, control and Bves/NDRG4-depleted epicardial cells move directionally (A'). On Bves/NDRG4-depleted ECM, control cells move directionally while Bves/NDRG4-depleted cells have poor directional persistence (A'; *$p < 0.01$). (B) Control epicardial cells fed medium lacking fibronectin move directionally on control ECM and fail to move directionally (B') on Bves/NDRG4-depleted ECM (*$p < 0.01$). This differs from A, in which controls overcome Bves/NDRG4-depleted ECM deficiency. (C) Biotin-labeled fibronectin deposition onto a glass surface is impaired in Bves/NDRG4-depleted cells compared with controls ($n = 7$ assays, **$p < 0.001$). (D, E) Epicardial cells internalize DyLight-550–labeled fibronectin (DyLight-FN) after a 1-h pulse. Endogenous Bves (D) and NDRG4 (E) colocalize with DyLight-FN on vesicular structures; boxes in merge denote digitally zoomed region. Optical slices, 1 AU; scale, 10 μm; n ≥ 50 cells/assay.

internalize and resecrete fibronectin present in the medium for use as a motility substrate. To test this hypothesis, we replated cells on matrix deposited by control or Bves/NDRG4-depleted cells. Motility assays were then performed in medium depleted of fibronectin (prepared as described by Danen, 2002). SC-treated cells moved in a directionally persistent manner on matrix produced by SC cells, as dynamic ECM secretion of internalized fibronectin was unnecessary on a well-formed matrix (Figure 7B). Conversely, in the absence of soluble fibronectin, control cells were unable to migrate persistently when plated on matrix produced in the absence of Bves and NDRG4 function (Figure 7, B and B'; SC cells on SC ECM, Supplemental Movie S13; SC cells on Bves/NDRG4-depleted ECM, Supplemental Movie S14). Thus the presence of fibronectin in the medium is required for control cells to overcome deficiencies in matrix produced by Bves/NDRG4-depleted cells (compare Figure 7, A' and B'). These data demonstrate that autocrine ECM deposition is necessary for persistent epicardial cell movement. Loss of cellular Bves and NDRG4 function disrupts this process.

We next directly tested whether Bves and NDRG4 regulate fibronectin internalization and/or deposition. Biotin-labeled fibronectin was added to the medium of control and Bves/NDRG4-depleted epicardial cell sheets after 24 h of culture in fibronectin-free medium. After 18 h, cells were removed from the plate as before, and the amount of biotin-labeled fibronectin present in the resulting autocrine-deposited ECM was quantified by streptavidin–horseradish peroxidase (HRP) enzyme-linked immunosorbent assay. Absorbance measurements demonstrated that Bves/NDRG4-depleted epicardial cells deposited fourfold less fibronectin than controls (Figure 7C). To visualize directly whether epicardial cells internalized fibronectin, we pulsed cells grown in fibronectin-depleted medium with DyLight 550-labeled fibronectin for 1 h (Figure 7, D and E). Under these conditions, internalized DyLight 550 fibronectin localized to vesicular compartments and colabeled with Bves and NDRG4 (Figure 7, D and E, respectively). Taken collectively, our studies demonstrate that internalization of soluble fibronectin into vesicles proceeds in the absence of Bves and NDRG4. Resecretion of this ECM component depends on their function in transport vesicles to promote directionally persistent migration.

Bves and NDRG4 mediate plasma membrane fusion of endosomal compartments

The present data demonstrate that Bves and NDRG4 mediate a critical cellular behavior, autocrine fibronectin recycling. In addition, Bves was previously implicated in exocytosis of many other cargoes (Hager and Bader, 2009). Because Bves is an integral plasma membrane protein, a likely mechanism regulated by Bves is vesicle docking, potentially via its binding partner VAMP3. Thus we tested whether

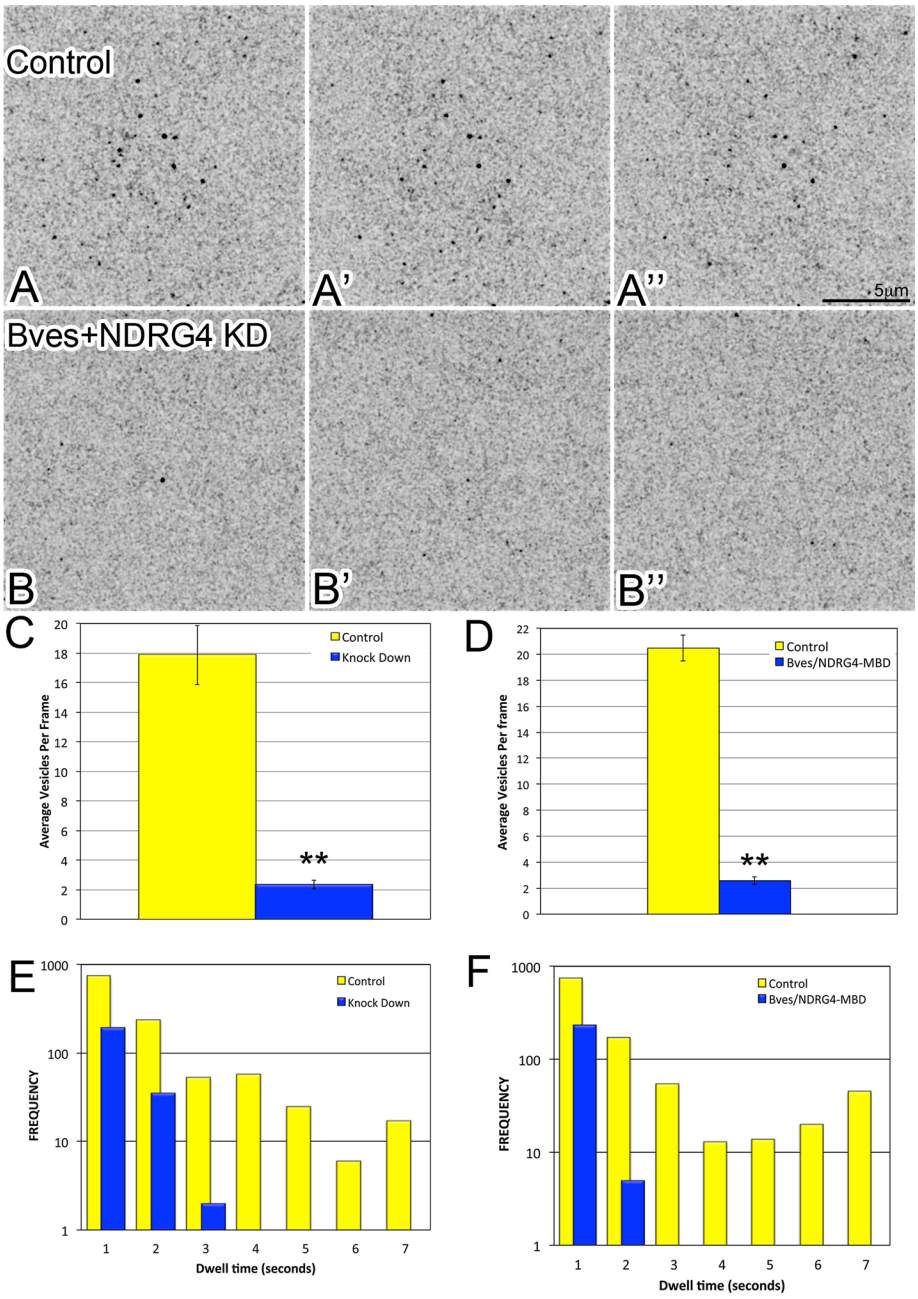

FIGURE 8: Bves/NDRG4 interaction is required for long-term exocytic vesicle docking at the plasma membrane. Three consecutive time-lapse TIRF microscopy images of control (A–A″) and Bves/NDRG4 (B–B″) knockdown cells transfected with Vamp3-GFP (black dots). Control cells contain numerous VAMP3 vesicles (C; yellow, 17.9) at the membrane over the time course, whereas Bves/NDRG4 (C; blue, 2.3) knockdown cells contain significantly fewer (**$p \leq 0.0001$) average vesicles per movie frame. Similarly, vector control–transfected cells contain significantly more vesicles per frame than Bves/NDRG4-treated cells (D; yellow, 20.6; blue, 2.6; **$p \leq 0.0001$). Quantification of dwell time separated into 1-s bins (E) reveals that vesicles in Bves/NDRG4-knockdown cells do not reside at the membrane as long as VAMP3 vesicles do in SC-treated cells. Dwell-time quantifications of cells coexpressing VAMP3-GFP and control myc-3tag vector (F, yellow) or Bv/N4-MBD (blue) plasmids indicate that vesicles do not reside at the membrane as long in the presence of Bv/N4-MBD; $n \geq 15$ movies per condition.

VAMP3 vesicle docking requires Bves and NDRG4. Control or Bves/NDRG4-depleted epicardial cells were transfected with VAMP3-GFP. Movement and docking of fluorescent vesicles was monitored at the basal cell surface with TIRF microscopy (Figure 8, A–B″; black spots indicate VAMP3-GFP–labeled vesicles at plasma membrane). In control cells, visualized best in real-time movies, VAMP3-GFP vesicles were numerous at the basal surface (Figure 8, A–A″; SC, Supplemental Movie S15; quantification in Figure 8C). Alternatively, Bves/NDRG4-depleted cells exhibited significantly decreased presence of VAMP3-GFP vesicles in this region (Figure 8, B–B″ and C; Bves/NDRG4 depleted, Supplemental Movie S15). Similar experiments, in which epicardial cells were cotransfected with VAMP3-GFP and vector control or Bv/N4-MBD plasmids, demonstrated significant loss of VAMP3-GFP at the basal surface, with disruption of Bves/NDRG4 binding (Figure 8D). In addition, quantification of dwell times (separated into 1-s bins, monitored up to 7 s) indicated that many VAMP3-GFP vesicles resided at the basal surface for prolonged periods in controls, which is indicative of membrane docking (Malarkey and Parpura, 2011). Of importance, the dwell times of vesicles in Bves/NDRG4-depleted cells were significantly reduced compared with controls (between 1 and 3 s, with the majority ≤2 s). This demonstrated that vesicles in Bves/NDRG4-depleted cells failed to dock at the cell surface (Figure 8E). Similarly, cotransfection of Bv/N4-MBD and VAMP3-GFP in epicardial cells led to impaired dwell times compared with Myc-3tag vector–transfected controls (most resided at membrane between 1 and 2 s; Figure 8F). Taken together, these data indicate that the Bves/NDRG4 interaction mediates docking of VAMP3-labeled vesicles.

DISCUSSION

Here we identify a critical protein/protein interaction between Bves and NDRG4 that influences epicardial cell movements. Careful characterization of Bves/NDRG4 interaction using multiple, complementary methodologies revealed an overlapping function. Bves and NDRG regulate directional persistence in migratory cells to mediate directionality of these movements. Cell/matrix recombination techniques determined that Bves and NDRG4 facilitate directional movement by regulating autocrine fibronectin recycling as a motility substrate. Finally, TIRF microscopy revealed that Bves/NDRG4 interaction regulates fusion of cell surface–bound vesicles. Together these findings explain how delivery of plasma membrane–bound and secreted cargoes are impaired with Bves loss of function. We propose that the Bves complex is a pivotal regulator of cell migration and adhesion by mediating cell surface cargo delivery of functional components. In this way, Bves may have broad influence on many cellular behaviors affecting development, repair, and cancer.

Bves and NDRG4 regulate overlapping cellular behaviors

Multiple independent studies demonstrated that loss of Bves or NDRG4 functions results in disruption of cell movement. For example, morpholino Bves knockdown impairs lamellipodial formation in *Xenopus* head mesoderm and NIH-3T3 cells (Smith *et al.*, 2008; Hager *et al.*, 2010), and expression of antisense NDRG4 RNA inhibits neurite outgrowth in PC12 neuronal cell lines (Ohki *et al.*, 2002). We determined that Bves is an essential regulator of persistent directional migration. Depletion of NDRG4 or inhibition of the Bves/NDRG4 interaction also randomizes cell movement. These findings may explain the previously reported errors in morphogenesis and wound healing seen with Bves loss of function, where directed cell movement is required for gastrulation and wound closure (Ripley *et al.*, 2004, 2006). In addition, Bves and NDRG4 are hypermethylated and down-regulated in multiple cancer cell types (Feng *et al.*, 2008; Melotte *et al.*, 2009; Schilling *et al.*, 2009; Kim *et al.*, 2010; Williams *et al.*, 2011), and overexpression of either gene inhibits migration in related cancers (Melotte *et al.*, 2009; Williams *et al.*, 2011). The present data suggest a mechanism through which these gene products mediate directed migration in these contexts. Future studies will identify the specific role(s) for autocrine ECM deposition in these diverse in vivo settings.

Bves and NDRG4 are essential for autocrine fibronectin recycling

Bves is important in the trafficking of cell/cell and cell/matrix adhesion molecules to the cell surface through interaction with diverse binding partners (Hager and Bader, 2009). Here we determined that Bves and NDRG4 specifically mediate movement of fibronectin via resecretion of endocytosed ECM. The initial uptake of fibronectin is not inhibited with loss of Bves or NDRG4 function. Indeed, large fibronectin and LAMP2 (late endosome) and Rab11 (recycling endosome) double-positive compartments are found in the cytoplasm of Bves- and/or NDRG4-depleted cells. This suggests that Bves and NDRG4 function downstream of internalization to promote fibronectin secretion from either late or recycling endosomes. Vesicle fusion assays demonstrate that inhibiting Bves/NDRG4 interaction specifically disrupts VAMP3-positive vesicle docking to the cell surface. Furthermore, Bves/NDRG4 disruption results in a reduction in biotin-labeled fibronectin moving from the medium to the insoluble matrix. Together these data confirm that cargo delivery requires Bves- and NDRG4-mediated vesicle fusion.

Of interest, Bves binds to VAMP3, a vesicle-SNARE protein regulating endosome–plasma membrane tethering. Bves does not regulate VAMP3 expression levels (Proux-Gillardeaux *et al.*, 2005; Hager *et al.*, 2010). This interaction was important for β1-integrin trafficking and cell–substrate adhesion. Our new data show that both Bves and NDRG4 regulate delivery of VAMP3-labeled vesicles. Collective studies suggest that fibronectin and its integrin receptors are recycled in the same endosomal pathway to promote efficient cell motility. Of note, other groups observed that fibronectin bound to α5β1-integrin traffics into late endosomal/lysosomal compartments, demonstrating that they are cotrafficked in other systems (Lobert *et al.*, 2010; Dozynkiewicz *et al.*, 2011). Of importance, in studies on cortactin, fibronectin trafficked through a late endosomal/lysosomal compartment before exocytosis (Sung *et al.*, 2011). Together these data implicate Bves and binding partners as critical components of the fibronectin/β1-integrin exocytic mechanism. Although autocrine ECM deposition has been observed in cancer cells, mouse embryonic fibroblasts, and, now, epicardial cell lines, further studies in additional models are required to generalize this mechanism.

Although NDRG4 is known to affect cell migration in cancer and other cell lines (Nishimoto *et al.*, 2003; Melotte *et al.*, 2009; Wang and Hill, 2009) and delivery of intracerebral neurotrophic factors in mice (Yamamoto *et al.*, 2011), the present study is the first to identify the mechanism by which NDRG4 directs this behavior. Collective data suggest that NDRG4 regulates trafficking in multiple contexts. Of interest, other NDRG-family proteins also participate in subcellular trafficking. NDRG1 is required for E-cadherin recycling, as well as myelin sheath maintenance and APO AI/AII lipid trafficking in Schwann cells (Hunter *et al.*, 2005; Berger *et al.*, 2006; Kachhap *et al.*, 2007; King *et al.*, 2011). NDRG2 is necessary for interleukin-10 secretion (Choi *et al.*, 2010). A caveat of the present study is that NDRG1–3 may also participate in Bves-dependent fibronectin recycling mechanisms. Thus we speculate that some overlap may exist, although other NDRG proteins were not identified in our split-ubiquitin screen. This is an exciting avenue for future research, as it would further generalize the Bves trafficking function (Melotte *et al.*, 2010).

Of interest, NDRG4 binds Bves in a domain that is not present in the other Popdc family proteins. The three members of the *Popeye* gene family contain many alternative splice variants for each family member and are tissue specifically enriched (Hager and Bader, 2009). A diverse array of trafficking events has been credited to *Popeye* gene products. It is possible that Popeye-family gene products vary in order to facilitate trafficking of different binding partners, as needed by the cellular context. Indeed, we observed that specifically disrupting Bves/NDRG4 interaction was relevant only to cell directionality and not to migration rate/distance. Because other Bves binding partners such as guanine nucleotide exchange factor T (Smith *et al.*, 2008) also regulate cell migration, we speculate that the array of splice variants could govern individual cellular behaviors by binding to different Bves interaction partners.

Fibronectin recycling supports cell directionality

The present data demonstrate that autocrine fibronectin recycling supports directionally persistent cell movement. One possible explanation for the requirement of ECM in promoting persistent motility is that spontaneous cell polarization facilitating cell migration is frequently unstable. Thus it might be stabilized by adhesion formation at the leading edge of cells by newly secreted ECM. Consistent with this idea, Bves inhibition results in lamellipodial and cell polarization defects (Hager and Bader, 2009; Hager *et al.*, 2010). At lower matrix concentrations or in a complex ECM environment (e.g., in vivo), direct deposition of ECM at the leading edge of cells might be the most efficient mechanism to stabilize newly formed lamellipodia and thus strengthen cell polarization within a brief time frame. Bves and NDRG4 have emerged as critical regulators linking cell autocrine ECM deposition and directional movement.

Directed cell migration, autocrine ECM deposition, and the epicardium

Epicardium produces fibronectin, which is abundant subjacent to its epithelial component, and adherence of epicardial integrin receptors to these substrates is critical for coronary artery formation (Manasek, 1969; Kalman *et al.*, 1995; Kwee *et al.*, 1995; Yang *et al.*, 1995; Sengbusch *et al.*, 2002; Nahirney *et al.*, 2003). The present study identifies a subcellular trafficking mechanism that facilitates fibronectin recycling and links this property to epicardial cell movement. These studies require important follow-up analyses using other in vitro cell systems and in vivo models. Yet we propose that autocrine fibronectin recycling supports de novo matrix production

to mediate epicardial sheet migration during the complex tissue interactions that regulate heart development. Thus, although the epicardium is noted for synthesis of ECM components, the mechanism of matrix deposition identified here cannot be overlooked in ongoing analyses of cell movement in development, disease, and repair.

MATERIALS AND METHODS

Quantification

For the assays described here, statistics were performed in Excel 2011 (Microsoft, Redmond, WA). The error bars represent SEM. Standard Student's *t* tests were used to determine significance. All compared images were equivalently adjusted in Photoshop CS5 (Adobe, San Jose, CA). For intensity profile quantification, the ImageJ straighten program was used to follow structures at a width of five pixels; these pixels were averaged for fluorescence intensity, and each channel was plotted together in Excel versus distance (micrometers). Progressive paths of epicardial cells after gene manipulation were gathered using ImageJ Manual Tracking and images were compiled in Photoshop.

Mice

C57Bl/6J mice were kept in 12-h light/dark cycles with ad libitum access to standard chow diets and water. Five wild-type dams were mated naturally, and plug dates were recorded. Dams were killed at embryonic day (E) 14.5, and embryonic hearts of offspring were fixed in paraformaldehyde overnight at 4°C. Hearts were cryoprotected in a sucrose gradient and then flash frozen in OCT (Tissue-Tek Sakura Finetek, Torrance, CA). Frozen hearts were sectioned in 10-µm slices. Hearts were rehydrated in phosphate-buffered saline (PBS), permeabilized with 0.25% PBS-TX100, blocked in 10% normal goat serum, and incubated with Bves and NDRG4 antibodies using standard methodologies. Images were captured with Leica TCS-SP5 confocal microscope system (Leica Microsystems, Solms, Germany). All experiments performed with murine models followed Institutional Animal Care and Use Committee guidelines.

Cell culture, antibodies, immunocytochemistry, and immunohistochemistry

Epicardial cell maintenance and processing was standard (Wada *et al.*, 2003). The dilutions and manufacturers of the antibodies were as follows: anti-Bves SB3 (1:1000; Smith and Bader, 2006), anti-NDRG4 (91:500, H00065009-M01; Novus Biologicals, Littleton, CO), anti-fibronectin (1:100, SC-9068; Santa Cruz Biotechnology, Dallas, TX); anti–glyceraldehyde-3-phosphate dehydrogenase (1:500, ab290; Abcam, Cambridge, UK), anti-GFP (1:500, 632375; Clonetech Laboratories, Mountain View, CA), anti-Myc (1:200, 631206; Clonetech), Rab4a/b (1:200, ab13252; Abcam), Rab11a (1:500; gift from James Goldenring, Vanderbilt University), EEA1 (1:200, 610457; BD Biosciences, San Jose, CA), Lamp1 (1:100, 555798; BD Biosciences), Lamp2 (1:100, ab18538; Abcam), Rab27a (1:200, ab55667, Abcam), Alexa Fluor 488, 568, and 647 (1:1000; Molecular Probes, Eugene, OR), and 4′,6-diamidino-2-phenylindole (1:10,000; Invitrogen Life Technologies; Grand Island, NY). Zenon immunoglobulin G labeling kits were used for direct labeling (Molecular Probes). Slide preparation for immunocytochemistry was standard (Smith and Bader, 2006). For immunohistochemistry, 10-µm slices of E14.5 murine hearts were cryosectioned onto charged slides. Tissue processing followed standard methodologies (Osler *et al.*, 2005; Smith and Bader, 2006). Images were captured with a Leica TCS-SP5 confocal microscope (Leica Microsystems), Zeiss LSM150 inverted confocal microscopes, (Carl Zeiss, AG, Jena, Germany), and the DeltaVision Platform (Applied Precision, Issaquah, WA). All microscopy was done in conjunction with the Cell Imaging Shared Resource and Epithelial Biology Center Imaging Resource of Vanderbilt University Medical Center.

Split ubiquitin screen

A split ubiquitin screen of murine Bves (NM_024285) against a mouse heart library was performed as previously described (Hager *et al.*, 2010). Murine NDRG4 transcript A (NM_001195006.1) was cloned into the pPR3-N vector and passed all nutrient drop-out selection tests against Bves.

Coimmunoprecipitation, GST pull down, and native immunoprecipitation

For coimmunoprecipitation, Bves, cloned into the pCMV-myc-3tag-4A vector (Agilent Technology, Santa Clara, CA), and NDRG4, cloned into the pEGFP-C1 vector (BD Biosciences), were exogenously expressed in COS-7 monkey kidney cells (ATCC, Manassas, VA) with Lipofectamine 2000 (Invitrogen Life Technologies). Lysates were harvested as previously described (Hager *et al.*, 2010) and coimmunoprecipitations performed per manufacturer's instructions using Profound c-Myc Tag IP/Co-IP Application Set (Thermo Scientific Pierce, Rockford, IL). Bves-GST truncation pull downs of NDRG4-GFP expressed in COS7 cells were performed as previously described (Smith *et al.*, 2008). For native immunoprecipitation, lysates from 10-cm plates of epicardial cells were pooled in M-PER Mammalian Protein Extraction Reagent (Thermo Scientific Pierce). Using BS_3, 20 µg of Bves SB3 or MF-20 antibodies were cross-linked to protein G Magnetic Dynabeads (Invitrogen Life Technologies). Dynabeads were washed in PBS-T, pH 7.4, and 250 µl of epicardial cell lysate was applied and rocked at 4°C for 2 h. Bound proteins were eluted in 1× Laemmli buffer and probed with NDRG4 antibodies via Western blotting, which was exposed with standard methodology (Hager *et al.*, 2010).

SPOTs analysis

A SPOTs membrane designed to the Bves C-terminus (residues 115–358) was synthesized (Sigma Genosys, Woodlands, TX), with each 13-mer peptide having a 10–amino acid overlap with neighboring peptides. NDRG4-EGFP or EGFP vector control lysates were exogenously expressed in COS7 cells, and lysates were collected using M-PER buffer. Standard bicinchoninic acid assays (Thermo Scientific Pierce) determined total protein concentration, and the SPOTs membrane was prepped and incubated in lysate as previously described (Kawaguchi *et al.*, 2008). The membrane was incubated with GFP antibodies overnight at 4°C. Antibody binding was visualized using standard chemiluminescence methodology, and the membrane was regenerated using dimethylformamide as previously described (Kramer and Schneider-Mergener, 1998). The region surrounding the minimal-binding Bves DNA sequence (BC132044.1; residues 292–330) was cloned into the pCMV-3tag-4a vector (#240198; Agilent Technologies), and in-frame ligation was confirmed via PCR, restriction enzyme dropout of the insert, and sequencing (in conjunction with the Vanderbilt University DNA Sequencing Facility). Overexpression of 10 µg of two separate clones was performed with nucleofection as described later. Expression efficiency and colocalization were ascertained by analyzing images gathered with the Delta Vision platform and confocal microscopes.

Modified Boyden chamber migration assay

Epicardial cells, 3.0×10^5 per experiment, were pelleted for 10 min at 1500 RPM in a desktop microcentrifuge and resuspended in 400 µl of 10% fetal bovine serum (FBS) plus penicillin/streptomycin (Life Technologies) in DMEM. The cells were seeded to the basket of an 8.0 µM cell culture insert (EMD Millipore, Billerica, MA) and placed in 600 µl of the same medium in a 24-well plastic culture dish (BD Biosciences). Cells were incubated for 4 h and processed with standard methods (Cross *et al.*, 2011). Phase images were captured on an Olympus BX60 microscope and Olympus HKH 027239 camera (Olympus, Center Valley, PA).

siRNA knockdown and rescue

Oligos were designed against the 3′UTR of Bves and NDRG4 (Sigma Custom Oligos, St. Louis, MO; Supplemental Figure S4). Nucleofection using the Nucleofector II Device (Lonza, Basel, Switzerland) was optimized in epicardial cells with a Cell Line Optimization Kit (Lonza VCO-1001N). Briefly, 5×10^5 epicardials in nucelofection solution L using nucleofector program A-033 had the highest transfection efficiency of pMAX-GFP DNA (>70%) and highest viability (>80%). Using this protocol, we applied three pooled Bves and/or NDRG4 siRNA oligos to epicardial cells at 100 nM each, as well as standard control oligos (SIC001; Sigma). Cells were incubated for 48 h and collected, and protein concentration was normalized to expression of the housekeeping gene cyclophilin via Western blot. Rescue constructs of Bves and NDRG4 pCMV-Myc-3tag-4 vector (Agilent Technology) lacked the siRNA target sequences and were stably expressed in epicardial cells via nucleofection, followed by 3 wk of G418 treatment. Cells were clonally sorted at the Nashville VA Medical Center Flow Cytometry Core, expanded, and then assayed with a Boyden chamber, as described earlier. Alternatively, Bves full-length or Bves-275 truncation constructs in pCMV-Myc-3tag-4 vector were transiently cotransfected with siRNA and assayed.

Live-imaging assays and analysis

Epicardial cells siRNA depleted for SC, Bves, and/or NDRG4 plasmid or treated with GFP-vector and CMV-myc-3tag-4 vector or Bv/N4-MBD were incubated for 24 h in standard medium and then split (5000 cells) into glass-bottom, 35-mm dishes (MatTek, Ashland, MA) either uncoated or coated in 10 µg/cm^2 fibronectin (F4759; Sigma) and incubated for 2 h. To monitor cell movements, differential interference contrast images were acquired with the DeltaVision Platform (Applied Precision) in a temperature-, humidity-, and CO_2-controlled weather station. Images were taken every 60 s with autofocus every 30th image. The movies were analyzed for distance, velocity, and directional persistence using ImageJ Cell Tracker software.

Cell-free ECM assays

Control or Bves/NDRG4-knockdown epicardial cells were seeded at 1×10^6 on MatTek dishes or 5×10^5/well of a four-well glass chamber slide (Thermo Scientific) and grown to confluence (48 h). A cell-free ECM was prepared by applying 20 mM ammonium hydroxide to the cells with vigorous rocking for 5 min. The cellular debris was washed away with H_2O (1×) and PBS (3×) for 5 min each, again with vigorous rocking. As a measure of properly produced ECM, directional persistence was compared between control cells in complete medium, Bves- and NDRG4-knockdown cells in complete medium, and control cells in fibronectin-depleted medium as a negative control, using the described live-cell directional persistence assay.

Fibronectin medium depletion and fibronectin internalization/deposition assays

To deplete the medium of fibronectin, FBS was purified over a disposable column using Gelatin Sepharose 4B beads (GE Healthcare, Fairfield, CT) according to the manufacturer's protocol and assayed for fibronectin depletion via Western blot. Gene-depleted cells maintained on glass MatTek dishes were fibronectin starved for 24 h. DyLight550 NHS ester- (Thermo Scientific Pierce) or sulfo-NHS-LC-LC-biotin-labeled fibronectin was incubated at 10 µg/ml for times specified in the text and as previously described (Sung *et al.*, 2011). Cells were washed 2× with complete medium and 3× with PBS for 5 min each and then were processed for immunofluorescence as before. For DiI labeling experiments, epicardial cells seeded at very low confluence on glass or 10 µg/cm^2 fibronectin were covered with 200 µl of Fast DiI (Molecular Probes; 5 µl DiI/1 ml 10% FBS DMEM), incubated for 35 min at 37°C, fixed with Formalin for 25 min, and processed for antibody labeling as described. For biotin-labeled deposition experiments, confluent fibronectin-starved cell sheets on 35-mm plastic dishes (Corning, Corning, NY) were fed biotin-FN for 48 h and a cell-free assay was performed as described earlier. Exposed ECM was conjugated to streptavidin-HRP overnight at 4°C (Thermo Scientific). The plates were washed with Tris-buffered saline/Tween 20, pH 8.0, 4× for 10 min each. Cells were exposed to TMB substrate (Thermo Scientific Pierce) for 25 min. Reactions were stopped with 2 M sulfuric acid and absorbance read per manufacturer's protocol.

Vesicle fusion docking assay

Epicardial cells transfected with standard control siRNA, Bves/NDRG4 siRNA, CMV-myc3tag-4 vector plasmid, or Bv/N4-MBD plasmid and VAMP3-GFP plasmid were plated on MatTek dishes for imaging. TIRF microscopy was performed using a Nikon TiE inverted microscope (Nikon,Tokyo, Japan) equipped with a Nikon TIRF illuminator and a 100×/1.49 numerical aperture objective in combination with a 1.5× Optivar (75 nm/pixel). Images were acquired at 30 frames/s using a Hamamatsu ImageEM-CCD camera driven by MetaMorph software (Molecular Devices, Sunnyvale, CA). ImageJ software was used to quantify the number or particles per movie frame, and SpeckleTrackerJ plug-in was used to quantify particle dwell times.

ACKNOWLEDGMENTS

We acknowledge J. Roland and the Epithelial Biology Center Imaging Resource, the Digestive Disease Research Center (P30DK058404), the Cell Imaging Shared Resource, the DNA Resources Core, and the DNA Sequencing Facility, Vanderbilt University, and the Nashville VA Flow Cytometry Core, Nashville, TN. A.M.W. and B.H.S. were supported by National Institutes of Health Grant 1R01GM075126, American Cancer Society Grant RSG-118085, and American Heart Association Grant-in-Aid 13GRNT16580020. E.C.B., P.M.M., H.A.H., and D.M.B. were supported by National Institutes of Health Grants 5T32 HL007411 and DK 83234-01

REFERENCES

Andrée B, Fleige A, Arnold HH, Brand T (2002). Mouse Pop1 is required for muscle regeneration in adult skeletal muscle. Mol Cell Biol 22, 1504–1512.

Andrée B, Hillemann T, Kessler-Icekson G, Schmitt-John T, Jockusch H, Arnold HH, Brand T (2000). Isolation and characterization of the novel Popeye gene family expressed in skeletal muscle and heart. Dev Biol 223, 371–382.

Bader D, Masaki T, Fischman DA (1982). Immunochemical analysis of myosin heavy chain during avian myogenesis in vivo and in vitro. J Cell Biol 95, 763–770.

Berger P, Niemann A, Suter U (2006). Schwann cells and the pathogenesis of inherited motor and sensory neuropathies (Charcot-Marie-Tooth disease). Glia 54, 243–257.
Choi S-C *et al*. (2010). NDRG2 is one of novel intrinsic factors for regulation of IL-10 production in human myeloid cell. Biochem Biophys Res Commun 396, 684–690.
Cross EE, Thomason RT, Martinez M, Hopkins CR, Hong CC, Bader DM (2011). Application of small organic molecules reveals cooperative TGFbeta and BMP regulation of mesothelial cell behaviors. ACS Chem Biol 6, 952–961.
Danen EHJ (2002). The fibronectin-binding integrins alpha5beta1 and alphavbeta3 differentially modulate RhoA-GTP loading, organization of cell matrix adhesions, and fibronectin fibrillogenesis. J Cell Biol 159, 1071–1086.
DiAngelo JR, Vasavada TK, Cain W, Duncan MK (2001). Production of monoclonal antibodies against chicken Pop1 (BVES). Hybrid Hybridomics 20, 377–381.
Dozynkiewicz MA *et al*. (2011). Rab25 and CLIC3 collaborate to promote integrin recycling from late endosomes/lysosomes and drive cancer progression. Dev Cell 22, 131–145.
Feng Q, Hawes SE, Stern JE, Wiens L, Lu H, Dong ZM, Jordan CD, Kiviat NB, Vesselle H (2008). DNA methylation in tumor and matched normal tissues from non-small cell lung cancer patients. Cancer Epidemiol Biomarkers Prev 17, 645–654.
Froese A *et al*. (2012). Popeye domain containing proteins are essential for stress-mediated modulation of cardiac pacemaking in mice. J Clin Invest 122, 1119–1130.
Hager HA, Bader DM (2009). Bves: ten years after. Histol Histopathol 24, 777–787.
Hager HA, Roberts RJ, Cross EE, Proux-Gillardeaux V, Bader DM (2010). Identification of a novel Bves function: regulation of vesicular transport. EMBO J 29, 532–545.
Harms BD, Bassi GM, Horwitz AR, Lauffenburger DA (2005). Directional persistence of EGF-induced cell migration is associated with stabilization of lamellipodial protrusions. Biophys J 88, 1479–1488.
Hunter M, Angelicheva D, Tournev I, Ingley E, Chan DC, Watts GF, Kremensky I, Kalaydjieva L (2005). NDRG1 interacts with APO A-I and A-II and is a functional candidate for the HDL-C QTL on 8q24. Biochem Biophys Res Commun 332, 982–992.
Iyer K, Bürkle L, Auerbach D, Thaminy S, Dinkel M, Engels K, Stagljar I (2005). Utilizing the split-ubiquitin membrane yeast two-hybrid system to identify protein-protein interactions of integral membrane proteins. Sci STKE 2005, pl3.
Kachhap SK, Faith D, Qian DZ, Shabbeer S, Galloway NL, Pili R, Denmeade SR, DeMarzo AM, Carducci MA (2007). The N-Myc down regulated gene1 (NDRG1) is a Rab4a effector involved in vesicular recycling of E-cadherin. PLOS ONE 2, e844.
Kalman F, Viragh S, Modis L (1995). Cell surface glycoconjugates and the extracellular matrix of the developing mouse embryo epicardium. Anat Embryol (Berl) 191, 451–464.
Kawaguchi M, Hager HA, Wada A, Koyama T, Chang MS, Bader DM (2008). Identification of a novel intracellular interaction domain essential for Bves function. PLOS ONE 3, e2261.
Kim M *et al*. (2010). Frequent silencing of Popeye domain-containing genes, BVES and POPDC3, is associated with promoter hypermethylation in gastric cancer. Carcinogenesis 31, 1685–1693.
King RHM *et al*. (2011). Ndrg1 in development and maintenance of the myelin sheath. Neurobiol Dis 42, 368–380.
Kramer A, Schneider-Mergener J (1998). Synthesis and screening of peptide libraries on continuous cellulose membrane supports. Methods Mol Biol 87, 25–39.
Kwee L, Baldwin HS, Shen HM, Stewart CL, Buck C, Buck CA, Labow MA (1995). Defective development of the embryonic and extraembryonic circulatory systems in vascular cell adhesion molecule (VCAM-1) deficient mice. Development 121, 489–503.
Lin S, Zhao D, Bownes M (2007). Blood vessel/epicardial substance (Bves) expression, essential for embryonic development, is down regulated by Grk/EFGR signalling. Int J Dev Biol 51, 37–44.
Lobert VH, Brech A, Pedersen NM, Wesche J, Oppelt A, Malerød L, Stenmark H (2010). Ubiquitination of alpha 5 beta 1 integrin controls fibroblast migration through lysosomal degradation of fibronectin-integrin complexes. Dev Cell 19, 148–159.
Malarkey EB, Parpura V (2011). Temporal characteristics of vesicular fusion in astrocytes: examination of synaptobrevin 2-laden vesicles at single vesicle resolution. J Physiol 589, 4271–4300.
Manasek FJ (1969). Embryonic development of the heart. II. Formation of the epicardium. J Embryol Exp Morphol 22, 333–348.
Melotte V *et al*. (2009). N-Myc downstream-regulated gene 4 (NDRG4): a candidate tumor suppressor gene and potential biomarker for colorectal cancer. J Natl Cancer Inst 101, 916–927.
Melotte V, Qu X, Ongenaert M, van Criekinge W, de Bruïne AP, Baldwin HS, van Engeland M (2010). The N-myc downstream regulated gene (NDRG) family: diverse functions, multiple applications. FASEB J 24, 4153–4166.
Nahirney P, Mikawa T, Fischman D (2003). Evidence for an extracellular matrix bridge guiding proepicardial cell migration to the myocardium of chick embryos. Dev Dyn 227, 511–523.
Neufeld EB *et al*. (2004). The ABCA1 transporter modulates late endocytic trafficking: insights from the correction of the genetic defect in Tangier disease. J Biol Chem 279, 15571–15578.
Nishimoto S, Tawara J, Toyoda H, Kitamura K, Komurasaki T (2003). A novel homocysteine-responsive gene, smap8, modulates mitogenesis in rat vascular smooth muscle cells. Eur J Biochem 270, 2521–2531.
Ohki T, Hongo S, Nakada N, Maeda A, Takeda M (2002). Inhibition of neurite outgrowth by reduced level of NDRG4 protein in antisense transfected PC12 cells. Brain Res Dev Brain Res 135, 55–63.
Okuda T, Higashi Y, Kokame K, Tanaka C, Kondoh H, Miyata T (2004). Ndrg1-deficient mice exhibit a progressive demyelinating disorder of peripheral nerves. Mol Cell Biol 24, 3949–3956.
Osler ME, Chang MS, Bader DM (2005). Bves modulates epithelial integrity through an interaction at the tight junction. J Cell Sci 118, 4667–4678.
Proux-Gillardeaux V, Gavard J, Irinopoulou T, Mege RM, Galli T (2005). Tetanus neurotoxin-mediated cleavage of cellubrevin impairs epithelial cell migration and integrin-dependent cell adhesion. Proc Natl Acad Sci USA 102, 6362–6367.
Qu X, Jia H, Garrity DM, Tompkins K, Batts L, Appel B, Zhong TP, Baldwin HS (2008). Ndrg4 is required for normal myocyte proliferation during early cardiac development in zebrafish. Dev Biol 317, 486–496.
Qu X, Zhai Y, Wei H, Zhang C, Xing G, Yu Y, He F (2002). Characterization and expression of three novel differentiation-related genes belong to the human NDRG gene family. Mol Cell Biochem 229, 35–44.
Reese DE, Zavaljevski M, Streiff NL, Bader D (1999). Bves: A novel gene expressed during coronary blood vessel development. Dev Biol 209, 159–171.
Ripley AN, Chang MS, Bader DM (2004). Bves is expressed in the epithelial components of the retina, lens, and cornea. Invest Ophthalmol Vis Sci 45, 2475–2483.
Ripley AN, Osler ME, Wright CVE, Bader D (2006). Xbves is a regulator of epithelial movement during early *Xenopus laevis* development. Proc Natl Acad Sci USA 103, 614–619.
Russ PK, Kupperman AI, Presley S-H, Haselton FR, Chang MS (2010). Inhibition of RhoA signaling with increased Bves in trabecular meshwork cells. Invest Ophthalmol Vis Sci 51, 223–230.
Russ PK, Pino CJ, Williams CS, Bader DM, Haselton FR, Chang MS (2011). Bves modulates tight junction associated signaling. PLOS ONE 6, e14563.
Schilling SH *et al*. (2009). NDRG4 is required for cell cycle progression and survival in glioblastoma cells. J Biol Chem 284, 25160–25169.
Sengbusch JK, He W, Pinco KA, Yang JT (2002). Dual functions of [alpha]4[beta]1 integrin in epicardial development: initial migration and long-term attachment. J Cell Biol 157, 873–882.
Smith T, Bader D (2006). Characterization of Bves expression during mouse development using newly generated immunoreagents. Dev Dyn 235, 1701–1708.
Smith TK, Hager HA, Francis R, Kilkenny DM, Lo CW, Bader DM (2008). Bves directly interacts with GEFT, and controls cell shape and movement through regulation of Rac1/Cdc42 activity. Proc Natl Acad Sci USA 105, 8298–8303.
Sung BH, Zhu X, Kaverina I, Weaver A M (2011). Cortactin controls cell motility and lamellipodial dynamics by regulating ECM secretion. Curr Biol 21, 1460–1469.
Vasavada TK, DiAngelo JR, Duncan MK (2004). Developmental expression of Pop1/Bves. J Histochem Cytochem 52, 371–377.
Wada AM, Reese DE, Bader DM (2001). Bves: prototype of a new class of cell adhesion molecules expressed during coronary artery development. Development 128, 2085–2093.

Wada AM, Smith TK, Osler ME, Reese DE, Bader DM (2003). Epicardial/mesothelial cell line retains vasculogenic potential of embryonic epicardium. Circ Res 92, 525–531.

Wang JF, Hill DJ (2009). Identification and action of N-myc downstream regulated gene 4 A2 in rat pancreas. J Endocrinol 201, 15–25.

Williams CS *et al.* (2011). BVES regulates EMT in human corneal and colon cancer cells and is silenced via promoter methylation in human colorectal carcinoma. J Clin Invest 121, 4056–4069.

Yamamoto H, Kokame K, Okuda T, Nakajo Y, Yanamoto H, Miyata T (2011). NDRG4 protein-deficient mice exhibit spatial learning deficits and vulnerabilities to cerebral ischemia. J Biol Chem 286, 26158–26165.

Yang JT, Rayburn H, Hynes RO (1995). Cell adhesion events mediated by alpha 4 integrins are essential in placental and cardiac development. Development 121, 549–560.

Zhou RH, Kokame K, Tsukamoto Y, Yutani C, Kato H, Miyata T (2001). Characterization of the human NDRG gene family: a newly identified member, NDRG4, is specifically expressed in brain and heart. Genomics 73, 86–97.